

Rapidity-Rank Structure of $p\bar{p}$ Pairs in Hadronic Z^0 Decays

DELPHI Collaboration

Abstract

The rapidity-rank structure of $p\bar{p}$ pairs is used to analyze the mechanism of baryon production in hadronic Z^0 decay. The relative occurrence of the rapidity-ordered configuration $pM\bar{p}$, where M is a meson, and that of $p\bar{p}$ adjacent pairs is compared. The data are found to be consistent with predictions from a mechanism producing adjacent-rank $p\bar{p}$ pairs, without requiring 'string-ordered' $pM\bar{p}$ configurations. An upper limit of 15% at 90% confidence is determined for the $pM\bar{p}$ contribution.

(Physics Letters B490(2000)61)

P.Abreu²², W.Adam⁵², T.Adye³⁸, P.Adzic¹², I.Ajinenko⁴⁴, Z.Albrecht¹⁸, T.Alderweireld², G.D.Alekseev¹⁷, R.Aleman⁵¹, T.Allmendinger¹⁸, P.P.Allport²³, S.Almehe²⁵, U.Amaldi^{9,29}, N.Amapane⁴⁷, S.Amato⁴⁹, E.G.Anassontzis³, P.Andersson⁴⁶, A.Andreazza⁹, S.Andringa²², P.Antilogus²⁶, W-D.Apel¹⁸, Y.Arnoud⁹, B.Åsman⁴⁶, J-E.Augustin²⁶, A.Augustinus⁹, P.Baillon⁹, P.Bambade²⁰, F.Barao²², G.Barbiellini⁴⁸, R.Barbier²⁶, D.Y.Bardin¹⁷, G.Barker¹⁸, A.Baroncelli⁴⁰, M.Battaglia¹⁶, M.Baubillier²⁴, K-H.Becks⁵⁴, M.Begalli⁶, A.Behrmann⁵⁴, P.Beilliere⁸, Yu.Belokopytov⁹, N.C.Benekos³³, A.C.Benvenuti⁵, C.Berat¹⁵, M.Berggren²⁴, D.Bertrand², M.Besancon⁴¹, M.Bigi⁴⁷, M.S.Bilenky¹⁷, M-A.Bizouard²⁰, D.Bloch¹⁰, H.M.Blom³², M.Bonesini²⁹, M.Boonekamp⁴¹, P.S.L.Booth²³, A.W.Borgland⁴, G.Borisov²⁰, C.Bosio⁴³, O.Botner⁵⁰, E.Boudinov³², B.Bouquet²⁰, C.Bourdarios²⁰, T.J.V.Bowcock²³, I.Boyko¹⁷, I.Bozovic¹², M.Bozzo¹⁴, M.Bracko⁴⁵, P.Branchini⁴⁰, R.A.Brenner⁵⁰, P.Bruckman⁹, J-M.Brunet⁸, L.Bugge³⁴, T.Buran³⁴, B.Buschbeck⁵², P.Buschmann⁵⁴, S.Cabrera⁵¹, M.Caccia²⁸, M.Calvi²⁹, T.Camporesi⁹, V.Canale³⁹, F.Carena⁹, L.Carroll²³, C.Caso¹⁴, M.V.Castillo Gimenez⁵¹, A.Cattai⁹, F.R.Cavallo⁵, V.Chabaud⁹, Ph.Charpentier⁹, P.Checchia³⁷, G.A.Chelkov¹⁷, R.Chierici⁴⁷, P.Chliapnikov^{9,44}, P.Chochula⁷, V.Chorowicz²⁶, J.Chudoba³¹, K.Cieslik¹⁹, P.Collins⁹, R.Contri¹⁴, E.Cortina⁵¹, G.Cosme²⁰, F.Cossutti⁹, H.B.Crawley¹, D.Crennell³⁸, S.Crepe¹⁵, G.Crosetti¹⁴, J.Cuevas Maestro³⁵, S.Czellar¹⁶, M.Davenport⁹, W.Da Silva²⁴, G.Della Ricca⁴⁸, P.Delpierre²⁷, N.Demaria⁹, A.De Angelis⁴⁸, W.De Boer¹⁸, C.De Clercq², B.De Lotto⁴⁸, A.De Min³⁷, L.De Paula⁴⁹, H.Dijkstra⁹, L.Di Ciaccio^{9,39}, J.Dolbeau⁸, K.Doroba⁵³, M.Dracos¹⁰, J.Drees⁵⁴, M.Dris³³, A.Duperrin²⁶, J-D.Durand⁹, G.Eigen⁴, T.Ekelof⁵⁰, G.Ekspong⁴⁶, M.Ellert⁵⁰, M.Elsing⁹, J-P.Engel¹⁰, M.Espirito Santo²², G.Fanourakis¹², D.Fassouliotis¹², J.Fayot²⁴, M.Feindt¹⁸, A.Ferrer⁵¹, E.Ferrer-Ribas²⁰, F.Ferro¹⁴, S.Fichet²⁴, A.Firestone¹, U.Flagmeyer⁵⁴, H.Foeth⁹, E.Fokitis³³, F.Fontanelli¹⁴, B.Franek³⁸, A.G.Frodesen⁴, R.Fruhwith⁵², F.Fulda-Quenzer²⁰, J.Fuster⁵¹, A.Galloni²³, D.Gamba⁴⁷, S.Gamblin²⁰, M.Gandelman⁴⁹, C.Garcia⁵¹, C.Gaspar⁹, M.Gaspar⁴⁹, U.Gasparini³⁷, Ph.Gavillet⁹, E.N.Gaziz³³, D.Gele¹⁰, L.Gerdyukov⁴⁴, N.Ghodbane²⁶, I.Gil⁵¹, F.Glege⁵⁴, R.Gokiel^{9,53}, B.Golob^{9,45}, G.Gomez-Ceballos⁴², P.Goncalves²², I.Gonzalez Caballero⁴², G.Gopal³⁸, L.Gorn¹, V.Gracco¹⁴, J.Grahl¹, E.Graziani⁴⁰, P.Gris⁴¹, G.Grosdidier²⁰, K.Grzelak⁵³, J.Guy³⁸, C.Haag¹⁸, F.Hahn⁹, S.Hahn⁵⁴, S.Haider⁹, A.Hallgren⁵⁰, K.Hamacher⁵⁴, J.Hansen³⁴, F.J.Harris³⁶, V.Hedberg^{9,25}, S.Heising¹⁸, J.J.Hernandez⁵¹, P.Herquet², H.Herr⁹, T.L.Hessing³⁶, J.-M.Heuser⁵⁴, E.Higon⁵¹, S-O.Holmgren⁴⁶, P.J.Holt³⁶, S.Hoorelbeke², M.Houlden²³, J.Hrubic⁵², M.Huber¹⁸, K.Huet², G.J.Hughes²³, K.Hultqvist^{9,46}, J.N.Jackson²³, R.Jacobsson⁹, P.Jalocha¹⁹, R.Janik⁷, Ch.Jarlskog²⁵, G.Jarlskog²⁵, P.Jarry⁴¹, B.Jean-Marie²⁰, D.Jeans³⁶, E.K.Johansson⁴⁶, P.Jonsson²⁶, C.Joram⁹, P.Juillot¹⁰, L.Jungermann¹⁸, F.Kapusta²⁴, K.Karafasoulis¹², S.Katsanevas²⁶, E.C.Katsoufis³³, R.Keranen¹⁸, G.Kernel⁴⁵, B.P.Kersevan⁴⁵, Yu.Khokhlov⁴⁴, B.A.Khomenko¹⁷, N.N.Khovanski¹⁷, A.Kiiskinen¹⁶, B.King²³, A.Kinvig²³, N.J.Kjaer⁹, O.Klapp⁵⁴, H.Klein⁹, P.Kluit³², P.Kokkinias¹², V.Kostioukhine⁴⁴, C.Kourkoumelis³, O.Kouznetsov⁴¹, M.Krammer⁵², E.Kriznic⁴⁵, Z.Krumstein¹⁷, P.Kubinec⁷, J.Kurowska⁵³, K.Kurvinen¹⁶, J.W.Lamsa¹, D.W.Lane¹, V.Lapin⁴⁴, J-P.Laugier⁴¹, R.Lauhakangas¹⁶, G.Leder⁵², F.Ledroit¹⁵, V.Lefebure², L.Leinonen⁴⁶, A.Leisos¹², R.Leitner³¹, J.Lemonne², G.Lenzen⁵⁴, V.Lepeltier²⁰, T.Lesiak¹⁹, M.Lethuillier⁴¹, J.Libby³⁶, W.Liebig⁵⁴, D.Liko⁹, A.Lipniacka^{9,46}, I.Lippi³⁷, B.Loerstad²⁵, J.G.Loken³⁶, J.H.Lopes⁴⁹, J.M.Lopez⁴², R.Lopez-Fernandez¹⁵, D.Loukas¹², P.Lutz⁴¹, L.Lyons³⁶, J.MacNaughton⁵², J.R.Mahon⁶, A.Maio²², A.Malek⁵⁴, T.G.M.Malmgren⁴⁶, S.Maltezos³³, V.Malychev¹⁷, F.Mandl⁵², J.Marco⁴², R.Marco⁴², B.Marechal⁴⁹, M.Margoni³⁷, J-C.Marin⁹, C.Mariotti⁹, A.Markou¹², C.Martinez-Rivero²⁰, F.Martinez-Vidal⁵¹, S.Marti i Garcia⁹, J.Masik¹³, N.Mastroiannopoulos¹², F.Matorras⁴², C.Matteuzzi²⁹, G.Matthiae³⁹, F.Mazzucato³⁷, M.Mazzucato³⁷, M.Mc Cubbin²³, R.Mc Kay¹, R.Mc Nulty²³, G.Mc Pherson²³, C.Meroni²⁸, W.T.Meyer¹, A.Miagkov⁴⁴, E.Migliore⁹, L.Mirabito²⁶, W.A.Mitaroff⁵², U.Mjoernmark²⁵, T.Moa⁴⁶, M.Moch¹⁸, R.Moeller³⁰, K.Moenig^{9,11}, M.R.Monge¹⁴, D.Moraes⁴⁹, X.Moreau²⁴, P.Morettini¹⁴, G.Morton³⁶, U.Mueller⁵⁴, K.Muenich⁵⁴, M.Mulders³², C.Mulet-Marquis¹⁵, R.Muresan²⁵, W.J.Murray³⁸, B.Mury¹⁹, G.Myatt³⁶, T.Myklebust³⁴, F.Naraghi¹⁵, M.Nassiakou¹², F.L.Navarria⁵, S.Navas⁵¹, K.Nawrocki⁵³, P.Negri²⁹, N.Neufeld⁹, R.Nicolaidou⁴¹, B.S.Nielsen³⁰, P.Niezurawski⁵³, M.Nikolenko^{10,17}, V.Nomokonov¹⁶, A.Nygren²⁵, V.Obraztsov⁴⁴, A.G.Olshevski¹⁷, A.Onofre²², R.Orava¹⁶, G.Orazi¹⁰, K.Osterberg¹⁶, A.Ouraou⁴¹, M.Paganoni²⁹, S.Paiano⁵, R.Pain²⁴, R.Paiva²², J.Palacios³⁶, H.Palka¹⁹, Th.D.Papadopoulou^{9,33}, K.Papageorgiou¹², L.Pape⁹, C.Parkes⁹, F.Parodi¹⁴, U.Parzefall²³, A.Passeri⁴⁰, O.Passon⁵⁴, T.Pavel²⁵, M.Pegoraro³⁷, L.Peralta²², M.Pernicka⁵², A.Perrotta⁵, C.Petridou⁴⁸, A.Petrolini¹⁴, H.T.Phillips³⁸, F.Pierre⁴¹, M.Pimenta²², E.Piotto²⁸, T.Podobnik⁴⁵, M.E.Pol⁶, G.Polok¹⁹, P.Poropat⁴⁸, V.Pozdniakov¹⁷, P.Privitera³⁹, N.Pukhaeva¹⁷, A.Pullia²⁹, D.Radojicic³⁶, S.Ragazzi²⁹, H.Rahmani³³, J.Rames¹³, P.N.Ratoff²¹, A.L.Read³⁴, P.Rebecchi⁹, N.G.Redaeli²⁹, M.Regler⁵², J.Rehn¹⁸, D.Reid³², R.Reinhardt⁵⁴, P.B.Renton³⁶, L.K.Resvanis³, F.Richard²⁰, J.Ridky¹³, G.Rinaudo⁴⁷, I.Ripp-Baudot¹⁰, O.Rohne³⁴, A.Romero⁴⁷, P.Ronchese³⁷, E.I.Rosenberg¹, P.Rosinsky⁷, P.Roudeau²⁰, T.Rovelli⁵, Ch.Royon⁴¹, V.Ruhmann-Kleider⁴¹, A.Ruiz⁴², H.Saarikko¹⁶, Y.Sacquin⁴¹, A.Sadovsky¹⁷, G.Sajot¹⁵, J.Salt⁵¹, D.Sampsonidis¹², M.Sannino¹⁴, Ph.Schwemling²⁴, B.Schwering⁵⁴, U.Schwickerath¹⁸, F.Scuri⁴⁸, P.Seager²¹, Y.Sedykh¹⁷, A.M.Segar³⁶, N.Seibert¹⁸, R.Sekulin³⁸, R.C.Shellard⁶, M.Siebel⁵⁴, L.Simard⁴¹, F.Simonetto³⁷, A.N.Sisakian¹⁷, G.Smadja²⁶, N.Smirnov⁴⁴, O.Smirnova²⁵, G.R.Smith³⁸, A.Sokolov⁴⁴, A.Sopczak¹⁸, R.Sosnowski⁵³, T.Spaso²², E.Spiriti⁴⁰, S.Squarcia¹⁴, C.Stanescu⁴⁰, S.Stanic⁴⁵, M.Stanitzki¹⁸, K.Stevenson³⁶, A.Stocchi²⁰, J.Strauss⁵², R.Strub¹⁰, B.Stugu⁴, M.Szczekowski⁵³, M.Szeptycka⁵³, T.Tabarelli²⁹, A.Taffard²³, F.Tegenfeldt⁵⁰, F.Terranova²⁹, J.Thomas³⁶, J.Timmermans³², N.Tinti⁵, L.G.Tkatchev¹⁷, M.Tobin²³, S.Todorova¹⁰, A.Tomaradze², B.Tome²², A.Tonazzo⁹, L.Tortora⁴⁰, P.Tortosa⁵¹, G.Transtromer²⁵, D.Treille⁹, G.Tristram⁸,

M.Trochimczuk⁵³, C.Troncon²⁸, M-L.Turluer⁴¹, I.A.Tyapkin¹⁷, S.Tzamarias¹², O.Ullaland⁹, V.Uvarov⁴⁴, G.Valenti^{9,5}, E.Vallazza⁴⁸, P.Van Dam³², W.Van den Boeck², J.Van Eldik^{9,32}, A.Van Lysebetten², N.van Remortel², I.Van Vulpen³², G.Vegni²⁸, L.Ventura³⁷, W.Venus^{38,9}, F.Verbeure², P.Verdier²⁶, M.Verlato³⁷, L.S.Vertogradov¹⁷, V.Verzi²⁸, D.Vilanova⁴¹, L.Vitale⁴⁸, E.Vlasov⁴⁴, A.S.Vodopyanov¹⁷, G.Voulgaris³, V.Vrba¹³, H.Wahlen⁵⁴, C.Walck⁴⁶, A.J.Washbrook²³, C.Weiser⁹, D.Wicke⁵⁴, J.H.Wickens², G.R.Wilkinson³⁶, M.Winter¹⁰, M.Witek¹⁹, G.Wolf⁹, J.Yi¹, O.Yushchenko⁴⁴, A.Zalewska¹⁹, P.Zalewski⁵³, D.Zavrtanik⁴⁵, E.Zevgolatakos¹², N.I.Zimin^{17,25}, A.Zintchenko¹⁷, Ph.Zoller¹⁰, G.C.Zucchelli⁴⁶, G.Zumerle³⁷

¹Department of Physics and Astronomy, Iowa State University, Ames IA 50011-3160, USA

²Physics Department, Univ. Instelling Antwerpen, Universiteitsplein 1, B-2610 Antwerpen, Belgium and IIHE, ULB-VUB, Pleinlaan 2, B-1050 Brussels, Belgium

and Faculté des Sciences, Univ. de l'Etat Mons, Av. Maistriau 19, B-7000 Mons, Belgium

³Physics Laboratory, University of Athens, Solonos Str. 104, GR-10680 Athens, Greece

⁴Department of Physics, University of Bergen, Allégaten 55, NO-5007 Bergen, Norway

⁵Dipartimento di Fisica, Università di Bologna and INFN, Via Irnerio 46, IT-40126 Bologna, Italy

⁶Centro Brasileiro de Pesquisas Físicas, rua Xavier Sigaud 150, BR-22290 Rio de Janeiro, Brazil and Depto. de Física, Pont. Univ. Católica, C.P. 38071 BR-22453 Rio de Janeiro, Brazil

and Inst. de Física, Univ. Estadual do Rio de Janeiro, rua São Francisco Xavier 524, Rio de Janeiro, Brazil

⁷Comenius University, Faculty of Mathematics and Physics, Mlynska Dolina, SK-84215 Bratislava, Slovakia

⁸Collège de France, Lab. de Physique Corpusculaire, IN2P3-CNRS, FR-75231 Paris Cedex 05, France

⁹CERN, CH-1211 Geneva 23, Switzerland

¹⁰Institut de Recherches Subatomiques, IN2P3 - CNRS/ULP - BP20, FR-67037 Strasbourg Cedex, France

¹¹Now at DESY-Zeuthen, Platanenallee 6, D-15735 Zeuthen, Germany

¹²Institute of Nuclear Physics, N.C.S.R. Demokritos, P.O. Box 60228, GR-15310 Athens, Greece

¹³FZU, Inst. of Phys. of the C.A.S. High Energy Physics Division, Na Slovance 2, CZ-180 40, Praha 8, Czech Republic

¹⁴Dipartimento di Fisica, Università di Genova and INFN, Via Dodecaneso 33, IT-16146 Genova, Italy

¹⁵Institut des Sciences Nucléaires, IN2P3-CNRS, Université de Grenoble 1, FR-38026 Grenoble Cedex, France

¹⁶Helsinki Institute of Physics, HIP, P.O. Box 9, FI-00014 Helsinki, Finland

¹⁷Joint Institute for Nuclear Research, Dubna, Head Post Office, P.O. Box 79, RU-101 000 Moscow, Russian Federation

¹⁸Institut für Experimentelle Kernphysik, Universität Karlsruhe, Postfach 6980, DE-76128 Karlsruhe, Germany

¹⁹Institute of Nuclear Physics and University of Mining and Metallurgy, Ul. Kawiora 26a, PL-30055 Krakow, Poland

²⁰Université de Paris-Sud, Lab. de l'Accélérateur Linéaire, IN2P3-CNRS, Bât. 200, FR-91405 Orsay Cedex, France

²¹School of Physics and Chemistry, University of Lancaster, Lancaster LA1 4YB, UK

²²LIP, IST, FCUL - Av. Elias Garcia, 14-1^o, PT-1000 Lisboa Codex, Portugal

²³Department of Physics, University of Liverpool, P.O. Box 147, Liverpool L69 3BX, UK

²⁴LPNHE, IN2P3-CNRS, Univ. Paris VI et VII, Tour 33 (RdC), 4 place Jussieu, FR-75252 Paris Cedex 05, France

²⁵Department of Physics, University of Lund, Sölvegatan 14, SE-223 63 Lund, Sweden

²⁶Université Claude Bernard de Lyon, IPNL, IN2P3-CNRS, FR-69622 Villeurbanne Cedex, France

²⁷Univ. d'Aix - Marseille II - CPP, IN2P3-CNRS, FR-13288 Marseille Cedex 09, France

²⁸Dipartimento di Fisica, Università di Milano and INFN-MILANO, Via Celoria 16, IT-20133 Milan, Italy

²⁹Dipartimento di Fisica, Univ. di Milano-Bicocca and INFN-MILANO, Piazza delle Scienze 2, IT-20126 Milan, Italy

³⁰Niels Bohr Institute, Blegdamsvej 17, DK-2100 Copenhagen Ø, Denmark

³¹IPNP of MFF, Charles Univ., Areal MFF, V Holesovickach 2, CZ-180 00, Praha 8, Czech Republic

³²NIKHEF, Postbus 41882, NL-1009 DB Amsterdam, The Netherlands

³³National Technical University, Physics Department, Zografou Campus, GR-15773 Athens, Greece

³⁴Physics Department, University of Oslo, Blindern, NO-1000 Oslo 3, Norway

³⁵Dpto. Física, Univ. Oviedo, Avda. Calvo Sotelo s/n, ES-33007 Oviedo, Spain

³⁶Department of Physics, University of Oxford, Keble Road, Oxford OX1 3RH, UK

³⁷Dipartimento di Fisica, Università di Padova and INFN, Via Marzolo 8, IT-35131 Padua, Italy

³⁸Rutherford Appleton Laboratory, Chilton, Didcot OX11 0QX, UK

³⁹Dipartimento di Fisica, Università di Roma II and INFN, Tor Vergata, IT-00173 Rome, Italy

⁴⁰Dipartimento di Fisica, Università di Roma III and INFN, Via della Vasca Navale 84, IT-00146 Rome, Italy

⁴¹DAPNIA/Service de Physique des Particules, CEA-Saclay, FR-91191 Gif-sur-Yvette Cedex, France

⁴²Instituto de Física de Cantabria (CSIC-UC), Avda. los Castros s/n, ES-39006 Santander, Spain

⁴³Dipartimento di Fisica, Università degli Studi di Roma La Sapienza, Piazzale Aldo Moro 2, IT-00185 Rome, Italy

⁴⁴Inst. for High Energy Physics, Serpukov P.O. Box 35, Protvino, (Moscow Region), Russian Federation

⁴⁵J. Stefan Institute, Jamova 39, SI-1000 Ljubljana, Slovenia and Laboratory for Astroparticle Physics,

Nova Gorica Polytechnic, Kostanjevska 16a, SI-5000 Nova Gorica, Slovenia,

and Department of Physics, University of Ljubljana, SI-1000 Ljubljana, Slovenia

⁴⁶Fysikum, Stockholm University, Box 6730, SE-113 85 Stockholm, Sweden

⁴⁷Dipartimento di Fisica Sperimentale, Università di Torino and INFN, Via P. Giuria 1, IT-10125 Turin, Italy

⁴⁸Dipartimento di Fisica, Università di Trieste and INFN, Via A. Valerio 2, IT-34127 Trieste, Italy

and Istituto di Fisica, Università di Udine, IT-33100 Udine, Italy

⁴⁹Univ. Federal do Rio de Janeiro, C.P. 68528 Cidade Univ., Ilha do Fundão BR-21945-970 Rio de Janeiro, Brazil

⁵⁰Department of Radiation Sciences, University of Uppsala, P.O. Box 535, SE-751 21 Uppsala, Sweden

⁵¹IFIC, Valencia-CSIC, and D.F.A.M.N., U. de Valencia, Avda. Dr. Moliner 50, ES-46100 Burjassot (Valencia), Spain

⁵²Institut für Hochenergiephysik, Österr. Akad. d. Wissensch., Nikolsdorfergasse 18, AT-1050 Vienna, Austria

⁵³Inst. Nuclear Studies and University of Warsaw, Ul. Hoza 69, PL-00681 Warsaw, Poland

⁵⁴Fachbereich Physik, University of Wuppertal, Postfach 100 127, DE-42097 Wuppertal, Germany

1 Introduction

Baryon production from hadronic Z^0 decays, as interpreted in string-fragmentation models, is pictured in Figure 1. Hadronisation results from breaks in the string formed from the colour-neutral system which stretches between the primary quarks [1]. Breaks occur between virtual flavour-neutral $q\bar{q}$ pairs, with mesons formed from string elements containing an adjacent q and \bar{q} . Baryons are thought to be formed when breaks occur between diquark-antidiquark pairs, the baryon being made from adjacent diquark and quark [2]. A baryon and an antibaryon emerge as adjacent particles in rank along the string (‘string-rank’), or possibly separated in rank with a mesonic state between them. Figure 1(a) represents the case where the diquark is assumed to have a sufficiently large binding energy that it acts like a fundamental unit. Another possibility is to produce an ‘effective diquark’ through a step-wise process where two $q\bar{q}$ pairs are created, as shown in Figure 1(b). In this case a mesonic state also can be produced between the baryon and antibaryon, seen in Figure 1(c). This has been referred to as the ‘popcorn effect.’

In this paper, a novel method, using the rapidity-rank structure of $p\bar{p}$ pairs, is used to study the mechanism of baryon production in hadronic Z^0 decay. A measurement of the relative frequency of occurrence of the rapidity-ordered configuration (i) $p M \bar{p}$, where M is a charged meson, and (ii) $p\bar{p}$ adjacent in rapidity, is made to determine the magnitude of the popcorn effect. This approach provides greater sensitivity than that used in previous studies [3].

2 Data Sample and Event Selection

This analysis is based on data collected with the DELPHI detector [4] at the CERN LEP collider in 1994 and 1995 at the Z^0 centre-of-mass energy. The charged-particle tracking information relies on three cylindrical tracking detectors (Inner Detector, Time Projection Chamber (TPC), and Outer Detector) all operating in a 1.2 T magnetic field.

The selection criteria for charged particles are: momentum above 0.3 GeV/c, polar angle between 15° and 165° , and track length above 30 cm. In addition, the impact parameters with respect to the beam axis and along the longitudinal coordinate at the origin, are required to be below 0.05 and 0.25 cm, respectively. These impact parameter cuts decrease the number of protons which result from secondary interactions in the detector. Also, protons from Λ and Σ decays are largely removed.

Hadronic events are selected by requiring at least three charged particle tracks in each event hemisphere, and a total energy of all charged particles exceeding 15 GeV. The number of hadronic events is ~ 2 million.

Charged particle identification is provided by a tagging procedure which combines Cherenkov angle measurement from the RICH detector with ionization energy loss measured in the TPC. Details on the particle identification can be found in reference [4]. In the present analysis, the combined-probability tag is required to be at the ‘standard’ level [4]. In addition, the polar angle for identified particles is restricted to be in the barrel region, between 47° and 133° .

3 Rapidity-Rank Configurations $p\bar{p}$ and $p M \bar{p}$

This analysis studies $p\bar{p}$ correlations in the rapidity variable with respect to the ‘thrust’ direction. The thrust direction approximates the directions of the primary q and \bar{q} ,

especially for two-jet events. The rapidity, y , of a given particle is defined as $\frac{1}{2} \ln((E + p_L)/(E - p_L))$, where p_L is the momentum component parallel to the thrust axis, and E is the energy calculated using the particle mass as determined from RICH and the measured momentum. The restriction is made that events have only ‘one p and one \bar{p} ’ in a given hemisphere. Hemispheres are defined, one for positive y and one for negative y , with respect to the thrust direction. Each hemisphere is considered independently. The number of events with this selection is 27.6 thousand. The background to this event sample can be determined from the number of events that have two p ’s or two \bar{p} ’s in a given hemisphere. These events, 10.1 thousand, result mainly from p or \bar{p} misidentifications and also from non-correlated baryon-antibaryon pairs (i.e., a p and \bar{p} from different $B\bar{B}$ pairs). This yields a 63% purity, $(27.6\text{k} - 10.1\text{k})/27.6\text{k}$, for the $p\bar{p}$ sample.

A study of events from Jetset 7.3 [5], including detector simulation, determined the $p\bar{p}$ pair detection efficiency to be $\sim 35\%$, and the $p\bar{p}$ pair purity to be $\sim 60\%$, consistent with the above-mentioned value. These values are nearly constant over the range of the analysis variable Δy_{min} defined later. The efficiency is computed from the ratio of Jetset $p\bar{p}$ pairs detected, to the total number of $p\bar{p}$ pairs generated. The purity is obtained from the ratio of Jetset $p\bar{p}$ pairs detected and congruous with a generated $p\bar{p}$ pair, to the total number of $p\bar{p}$ pairs detected.

The charged particles in each event are ordered according to their rapidity values as defined above. The rapidity-rank is defined as the position that a particle has in the rapidity chain. In the following, two types of rapidity-rank configurations for $p\bar{p}$ pairs are considered, and are shown in Figure 2. The first is when the p and \bar{p} are adjacent in rapidity (ranks differ by one unit). The second is when the p and \bar{p} have one or more mesons between them. The number of mesons is restricted to be at most three (the ranks differ by two to four units). This reduces the probability that the p and \bar{p} may have come from different baryon-antibaryon pairs. It should be noted that the rapidity configurations only approximately portray the string-rank patterns as shown in Figure 1. This is because of the softness of the fragmentation function and of resonance decays which can mix the rapidity-ranks.

Since adjacent particles separated by a small rapidity gap have a high probability to have ‘crossed-over’ (reversed rank), this study is performed as a function of the rapidity gap size. For $p\bar{p}$ adjacent pairs, the concern is that a meson close in rapidity to the p or \bar{p} may have crossed-over from an original ‘string position’ which was between the $p\bar{p}$ pair. Correspondingly, for the $p M \bar{p}$ configuration, a meson on the outside of a $p\bar{p}$ pair on the ‘string’ may have crossed-over to be between the p and \bar{p} in the rapidity variable.

To determine the relative amount of $p\bar{p}$ and $p M \bar{p}$ configurations in the data the following ratio is calculated:

$$\mathcal{R}(\Delta y_{min}) = N(p M \bar{p}) / (N(p\bar{p}) + N(p M \bar{p})), \quad (1)$$

where $N(p\bar{p})$ and $N(p M \bar{p})$ represent the number of rapidity-rank configurations of each type in the data sample, and are implicitly a function of Δy_{min} , defined as follows. For the $p\bar{p}$ case, Figure 2(a), Δy_{min} is defined as the absolute rapidity difference between the nearest adjacent meson to either p or \bar{p} , whichever is smaller. In the $p M \bar{p}$ case, Figure 2(b), Δy_{min} is defined as the absolute rapidity difference between either p or \bar{p} and the particle in-between them, whichever is smaller. If there is more than one particle in-between, then the particle which is closest to being in the exact middle of the $p\bar{p}$ pair (and therefore least likely to have crossed over) is the one considered. With these definitions for Δy_{min} , the probability that a given rapidity configuration will represent the actual rank order on the string will be enhanced as Δy_{min} is made larger.

If the production of p and \bar{p} are correlated, the rapidity gaps between a $p\bar{p}$ pair are expected to be smaller than the gaps external to the pair. In the present data the average size of rapidity gaps between the p and \bar{p} for the $pM\bar{p}$ case (0.18 units) is $\sim 2/3$ the size of the adjacent rapidity gaps for the $p\bar{p}$ case (0.26 units). To put the two cases on a more equal footing, the definition of Δy_{min} for the $p\bar{p}$ case includes a multiplicative factor of $2/3$. This is arbitrary but it provides for a better balance of the two contributions when studying the ratio \mathcal{R} over a range of Δy_{min} . Excluded from the analysis are events where the particle with the largest rank (i.e., smallest rapidity) is a p or \bar{p} . This is to avoid the possibility that a low momentum particle may not have been detected (or reconstructed) and could have formed a small Δy_{min} that was not considered. The above treatments are applied to both data and model.

The ratio $\mathcal{R}(\Delta y_{min})$ for the data is plotted in Figure 3, as solid circles. Also shown are the predictions from Jetset 7.3 for the case when the relative fraction of the $pM\bar{p}$ string-rank configuration is zero and when it is 100%, indicated by open circles and squares, respectively. The errors are statistical. A background subtraction of like-sign pairs (pp and $\bar{p}\bar{p}$) has been applied to the data and model to remove contributions from uncorrelated baryon pairs and from particle misidentifications. The possible effect of variations (of order $\pm 30\%$) in the fraction of protons coming from resonances (like Deltas) was investigated, and found to be negligible. Standard DELPHI detector simulation along with charged particle reconstruction and hadronic event selection are applied to the events from Jetset 7.3 with parameters tuned as in reference [6]. Since Jetset was run with a 50% popcorn contribution, $p\bar{p}$ pairs were separated into string-rank $pM\bar{p}$ (popcorn) and $p\bar{p}$ (non-popcorn) components using the information on rank-order stored with the Monte-Carlo events. The prediction for the case with no contribution from $pM\bar{p}$ is seen to fall for large Δy_{min} , as expected. The case with 100% contribution might be thought to rise to the maximum value 1.0, but it flattens out possibly because contributions, for example, from $p\bar{p}$ pairs with a $\pi^0('s)$ in between become relatively more important for large Δy_{min} . As seen in Figure 3, the data are consistent with *no* contribution (or little) from $pM\bar{p}$ string configurations. The χ^2 between data and model was calculated as a function of the relative amount of $p\bar{p}$ and $pM\bar{p}$ configurations. The χ^2 is minimum over the range below 5% popcorn contribution; and, an upper-limit contribution of 15% is determined at 90% confidence level.

For completeness, the distributions, $N(p\bar{p})$ and $N(pM\bar{p})$, of the number of rapidity-rank configurations of each type as a function of Δy_{min} , are displayed in Figure 4. The data are shown by the solid circles. The predictions for the case when the relative fraction of the $pM\bar{p}$ string-rank configuration is zero and when it is 100%, are indicated by open circles and squares, respectively. In accord with the analysis above, consistency between the data and the prediction for no-popcorn is evident for these distributions.

4 The $p\bar{p}$ Rapidity Difference

Previous studies of baryon-antibaryon (in particular, $\Lambda\bar{\Lambda}$) rapidity correlations have claimed evidence for the popcorn effect [3]. In these studies, distributions of the $\Lambda\bar{\Lambda}$ rapidity difference were compared to predictions from the string-model Jetset. To test the sensitivity of this method for the $p\bar{p}$ case, the distribution of the $p\bar{p}$ rapidity difference, $\Delta y(p\bar{p})$, for the data was compared to the Jetset predictions for 100% popcorn and for no-popcorn contribution, as shown in Figure 5. The thrust value was required to be greater than 0.96. A background subtraction of like-sign pairs (pp and $\bar{p}\bar{p}$) has been applied to the data and model. The all-popcorn assumption yields a mean value for

$\Delta y(p\bar{p})$ that is 11% larger than that for no-popcorn; without the thrust requirement the difference is 5.5%. These values are in accordance with what is predicted in reference [7]. Even though this method is clearly not as sensitive as the one above-mentioned, it can be seen that the data prefer the no-popcorn prediction. The difference between the present result and that from $\Lambda\bar{\Lambda}$ experiments might indicate the importance of dynamical effects not incorporated in Jetset or simply the inadequacy of the popcorn model, although no firm conclusion can be drawn yet.

5 Conclusions

The rapidity-rank structure of $p\bar{p}$ pairs was used to analyze the mechanism of baryon production in hadronic Z^0 decay. By comparing the relative occurrence in the data of the rapidity-ordered configuration $pM\bar{p}$, where M is a meson, to that of $p\bar{p}$ adjacent pairs with predictions from Jetset, it is found that the data can be explained without requiring ‘string-ordered’ $pM\bar{p}$ configurations. The production of adjacent-rank $p\bar{p}$ pairs is sufficient to describe the data.

Acknowledgements

We are greatly indebted to our technical collaborators, to the members of the CERN-SL Division for the excellent performance of the LEP collider, and to the funding agencies for their support in building and operating the DELPHI detector.

We acknowledge in particular the support of

Austrian Federal Ministry of Science and Traffics, GZ 616.364/2-III/2a/98,

FNRS-FWO, Belgium,

FINEP, CNPq, CAPES, FUJB and FAPERJ, Brazil,

Czech Ministry of Industry and Trade, GA CR 202/96/0450 and GA AVCR A1010521,

Danish Natural Research Council,

Commission of the European Communities (DG XII),

Direction des Sciences de la Matière, CEA, France,

Bundesministerium für Bildung, Wissenschaft, Forschung und Technologie, Germany,

General Secretariat for Research and Technology, Greece,

National Science Foundation (NWO) and Foundation for Research on Matter (FOM),

The Netherlands,

Norwegian Research Council,

State Committee for Scientific Research, Poland, 2P03B06015, 2P03B1116 and SPUB/P03/178/98,

JNICT-Junta Nacional de Investigação Científica e Tecnológica, Portugal,

Vedecka grantova agentura MS SR, Slovakia, Nr. 95/5195/134,

Ministry of Science and Technology of the Republic of Slovenia,

CICYT, Spain, AEN96-1661 and AEN96-1681,

The Swedish Natural Science Research Council,

Particle Physics and Astronomy Research Council, UK,

Department of Energy, USA, DE-FG02-94ER40817.

References

- [1] B. Andersson, G. Gustafson, G. Ingelman and T. Sjöstrand, Phys. Rep. **97** (1983) 31.
- [2] A. Casher, H. Neuberger, and S. Nussinov, Phys. Rev. **D20** (1979) 179;
 U.P. Sukhatme, K.E. Lassila and R. Orava, Phys. Rev. **D25** (1982) 2975;
 T. Meyer, Z. Phys. **C12** (1982) 77;
 B. Andersson, G. Gustafson, G. Ingelman and T. Sjöstrand, Z. Phys. **C13** (1982) 361;
 A. Bartl, H. Fraas and W. Majerotto, Phys. Rev. **D26** (1982) 1061;
 A. Breakstone, et al., Z. Phys. **C28** (1985) 335;
 A. Breakstone, et al., Z. Phys. **C36** (1987) 567;
 M. Szczekowski, Int. J. Mod. Phys. **A4** (1989) 3985;
 M. Anselmino, E. Predazzi, S. Ekelin, S. Fredriksson and D.B. Lichtenberg, Rev. Mod. Phys. **65** (1993) 1199;
 P. Edén and G. Gustafson, Z. Phys. **C75** (1997) 41.
- [3] H. Aihara, et al., Phys. Rev. Lett. **55** (1985) 1047;
 OPAL Coll., P.D. Acton et al., Phys. Lett. **B305** (1993) 415;
 DELPHI Coll., P. Abreu et al., Phys. Lett. **B318** (1993) 249;
 ALEPH Coll., D. Buskulic et al., Z. Phys. **C64** (1994) 361;
 ALEPH Coll., D. Buskulic et al., Z. Phys. **C71** (1996) 357;
 DELPHI Coll., P. Abreu et al., Phys. Lett. **B416** (1998) 247;
 OPAL Coll., G. Abbiendi et al., CERN-EP/98-114, accepted by Eur. Phys. J. **C**.
- [4] DELPHI Coll., P. Aarnio et al., Nucl. Instr. and Meth. **A303** (1991) 233;
 DELPHI Coll., P. Abreu et al., Nucl. Instr. and Meth. **A378** (1996) 57;
 DELPHI Coll., P. Aarnio et al., Phys. Lett. **B240** (1990) 271.
- [5] T. Sjöstrand and M. Bengtsson, Comp. Phys. Comm. **43** (1987) 367;
 T. Sjöstrand, CERN-TH.6488/92, May 1992, Revised Sept. 1992.
- [6] DELPHI Coll., P. Abreu et al., Z. Phys. **C73** (1996) 11.
- [7] B. Anderson, G. Gustafson and T. Sjöstrand, Phys. Scripta **32** (1985) 574.

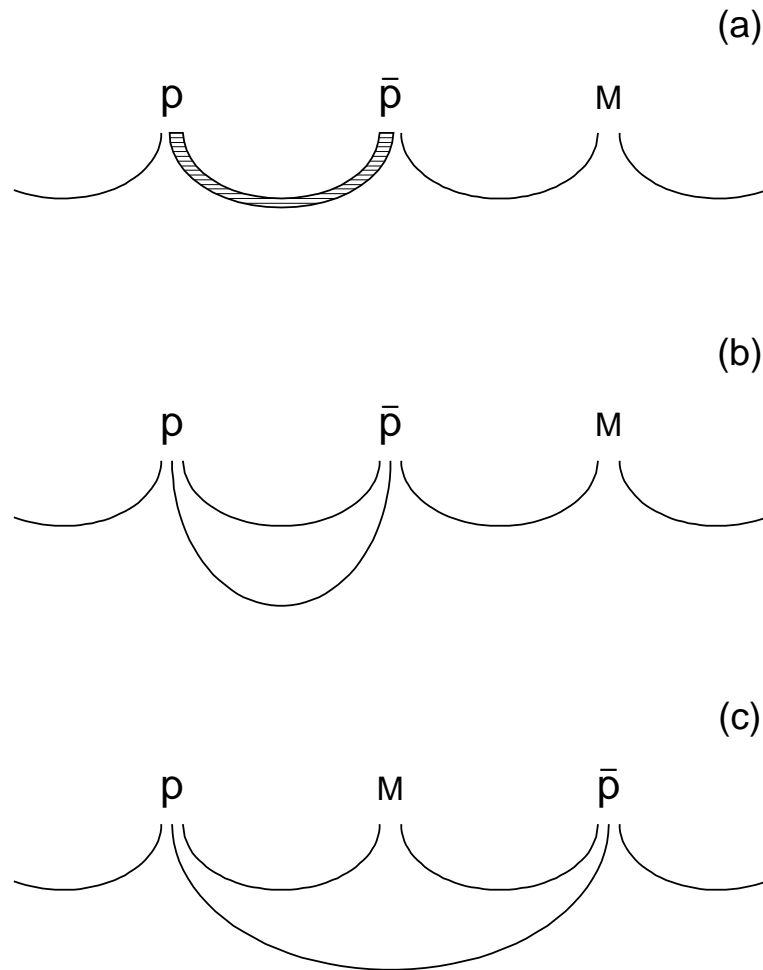


Figure 1: Illustration of $p\bar{p}$ production in the string model. Each line represents a $q\bar{q}$ pair produced from potential energy in the string. (a) Production by a diquark-antidiquark pair (shown shaded) acting as a fundamental unit. (b) Through a step-wise process with two $q\bar{q}$ pairs forming an effective diquark-antidiquark pair. (c) Step-wise production with a mesonic state formed between the $p\bar{p}$ pair (referred to as the popcorn effect).

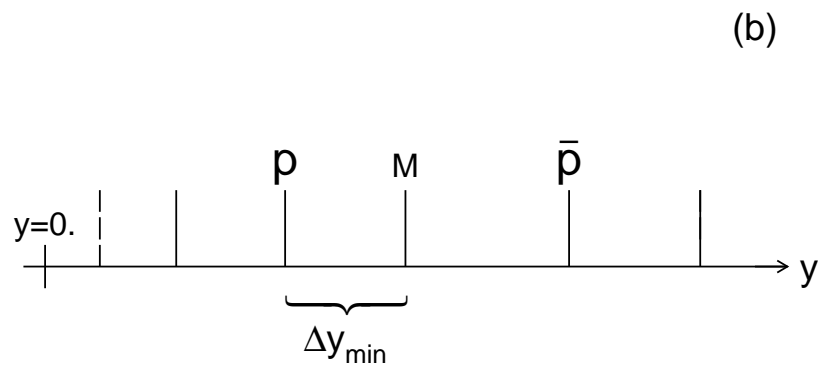
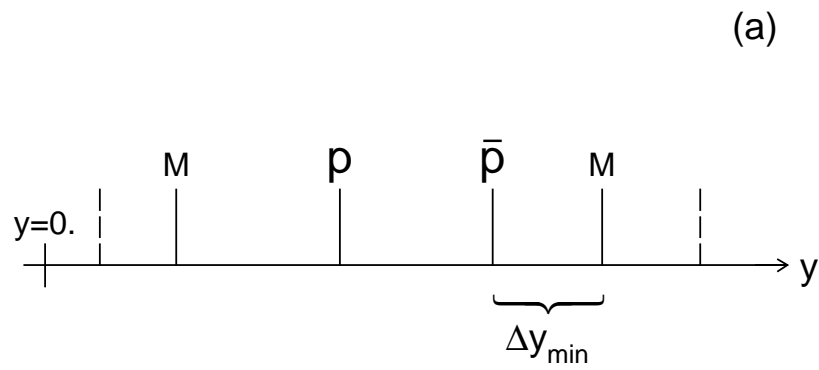


Figure 2: (a) An event hemisphere configuration with p and \bar{p} adjacent in rapidity. The rapidity-gap, Δy_{min} , indicates the distance to the nearest particle external to the $p\bar{p}$ pair. (b) An event configuration with a particle, M , between the p and \bar{p} . The rapidity-gap, Δy_{min} , denotes the distance of the particle, M , to the nearest of p or \bar{p} .

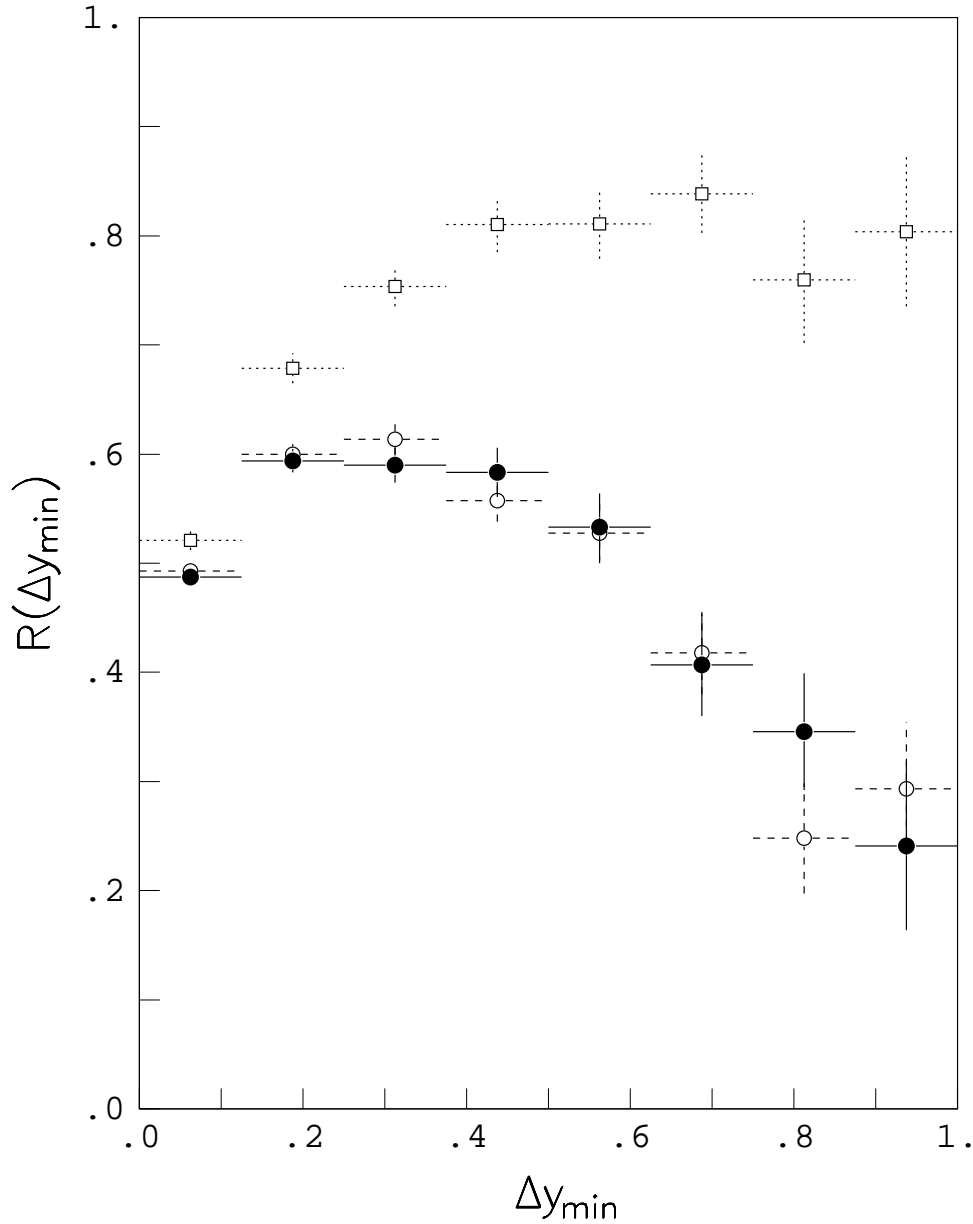


Figure 3: The relative amount, $\mathcal{R}(\Delta y_{min})$, of the $p M \bar{p}$ configuration as a function of Δy_{min} . The data points are indicated by solid circles. The predictions from Jetset for two cases: no contribution from the popcorn effect (open circles) and all popcorn effect (open squares).

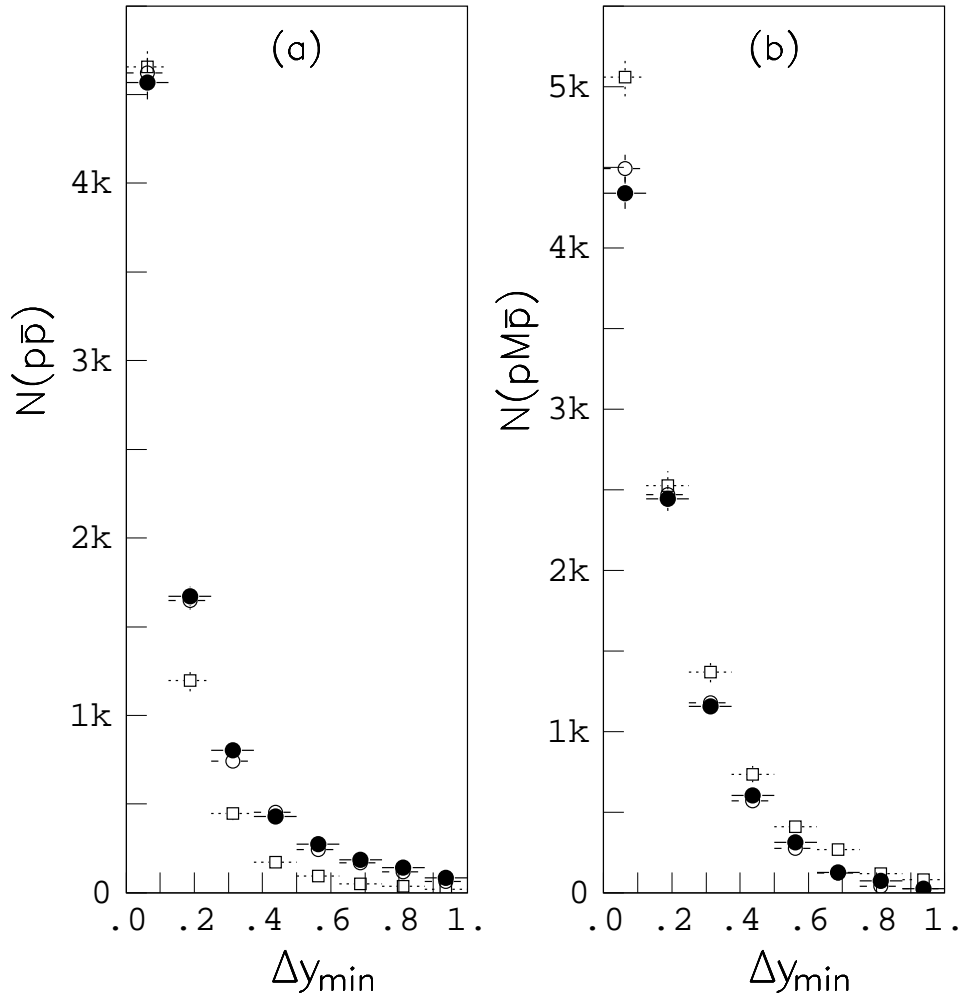


Figure 4: Distributions, $N(p\bar{p})$ and $N(pM\bar{p})$, of the number of rapidity-rank configurations of each type as a function of Δy_{\min} , in (a) and (b), respectively. The data points are indicated by solid circles. The predictions from Jetset for two cases: no contribution from the popcorn effect (open circles) and all popcorn effect (open squares).

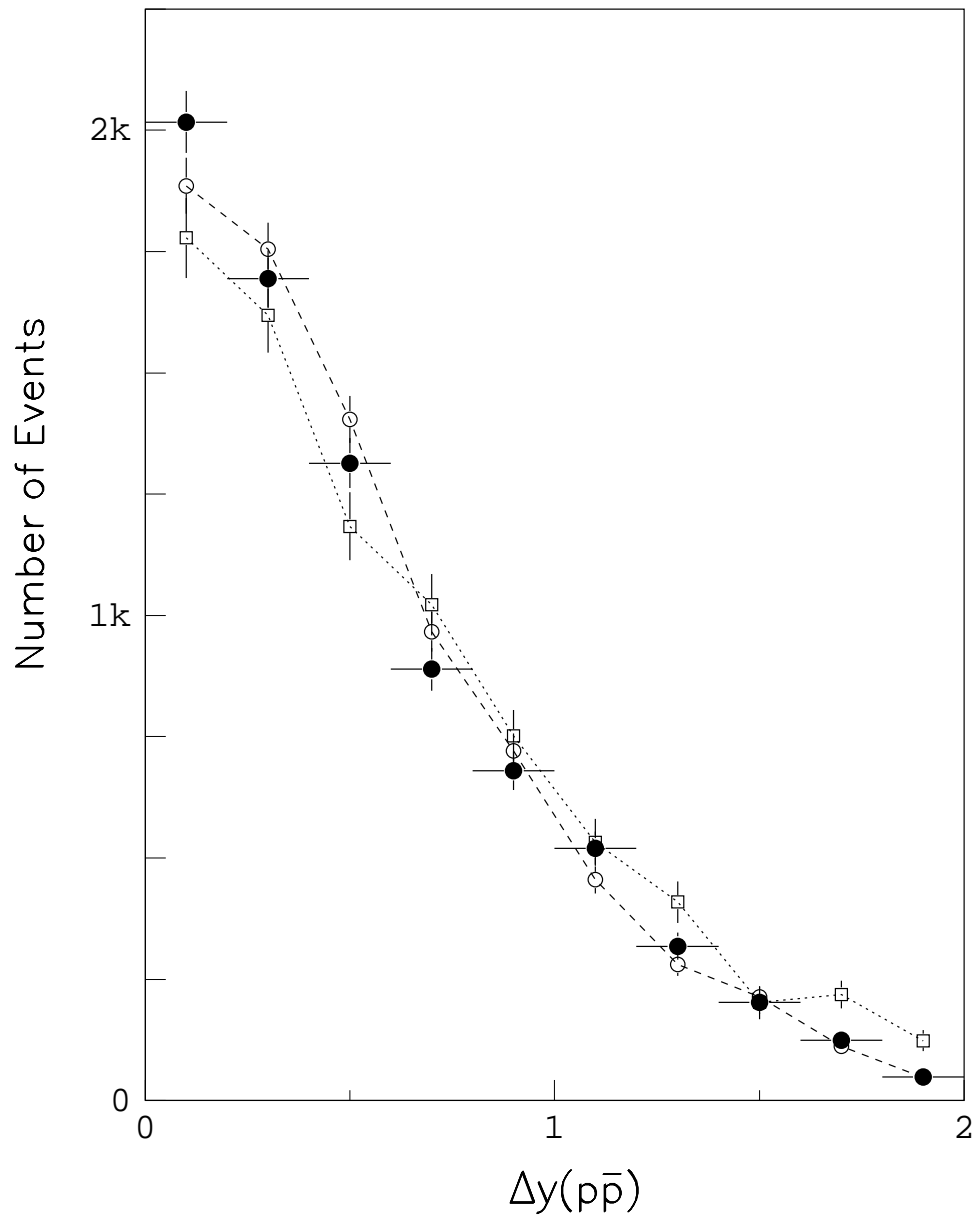


Figure 5: The distribution of $\Delta y(p\bar{p})$ for the data (solid circles), and the predictions of Jetset for no-contribution from the popcorn effect (open circles), and for an all-popcorn effect (open squares).